Germanium-on-Silicon Mid-Infrared Arrayed Waveguide Grating Multiplexers

Aditya Malik, Muhammad Muneeb, Shibnath Pathak, *Student Member, IEEE*, Yosuke Shimura, Joris Van Campenhout, *Member, IEEE*, Roger Loo, and Gunther Roelkens, *Member, IEEE*

***Abstract*— In this letter, we describe the use of a germanium-on-silicon waveguide platform to realize an arrayed waveguide grating (AWG) operating in the 5 μm wavelength range, which can be used as a wavelength multiplexer for mid-infrared (midIR) light engines or as the core element of a midIR spectrometer. Ge-on-Si waveguide losses in the range 2.5–3.5 dB/cm for TE polarized light and 3–4 dB/cm for TM polarized light in the 5.15–5.4 μm wavelength range are reported. A 200 GHz channel spacing 5-channel AWG with an insertion loss/crosstalk of 2.5/3.1 dB and 20/16 dB for TE and TM polarization, respectively, is demonstrated.**

***Index Terms*— Mid-infrared, arrayed waveguide gratings.**

I. Introduction

THE mid-infrared (midIR) wavelength range (3–12 μm) is of strong interest for spectroscopic sensing applications [1]. The main reason behind this interest is the fact that many gases have strong and specific absorption features in this wavelength range allowing non-contact detection of these gas species. The advent of quantum cascade lasers (QCL) and interband cascade lasers (ICLs) has enabled the realization of compact and relatively cheap mid-infrared coherent light sources based on epitaxially grown semiconductors, unlocking a broad range of applications. Typically, single wavelength distributed feedback (DFB) lasers are used, which can be thermally tuned over a narrow wavelength range. In order to extend the operational wavelength range of such mid-infrared emitters, arrays of such DFB devices have been realized, in which each DFB has a different emission wavelength [2]. In order to have access to this extended wavelength range in a single diffraction limited beam, a wavelength multiplexer should be used. Such multiplexers have been realized using free-space optical components [3]. However, in order to make a rugged, compact and cheap mid-infrared light engine, an integrated wavelength multiplexer that can be butt-coupled to the DFB laser array is of interest. On the other hand the spectroscopic analysis of midIR emission is also of interest in several applications. Also here, an integrated wavelength demultiplexer can be used as the core element of such a spectrometer. To realize such an integrated wavelength (de)multiplexer several waveguide platforms can be considered. For telecom wavelengths, silicon-on-insulator (SOI) is now a standard waveguide platform, which is mostly related to the fact that CMOS fabrication tools can be used to realize these waveguide circuits. However, it is known that beyond 3.8 μm, the SiO_2 buffer layer starts absorbing heavily [4], which therefore limits the use of SOI for spectroscopic sensing applications to below 4 μm wavelength [5]. In recent literature, several waveguide platforms have been proposed for the mid-infrared wavelength range as discussed in detail in [4]. There have been reports on germanium-on-silicon waveguides [6], free-standing silicon waveguides [7] and silicon-on-sapphire waveguides [8]. Germanium-on-silicon seems to be an interesting waveguide platform for the mid-infrared because of its compatibility with CMOS pilot lines and its relatively straightforward fabrication technique when compared with free-standing Si waveguides. Silicon-on-sapphire waveguide circuits can make use of a higher refractive index contrast compared to germanium-on- silicon, however the sapphire limits the transparency window to 5.5 μm. Given the large transparency window of germanium (up to 14 μm), the Ge-on-Si platform should allow implementing many optical functions over the complete mid-infrared wavelength range. Also, the lower index contrast on the germanium-on-silicon waveguide platform allows for a higher efficiency interfacing of the waveguide circuit with the outside world (i.e. QCL/ICL lasers). Therefore, in this letter we elaborate on the realization of germanium-on-silicon arrayed waveguide gratings as wavelength (de)multiplexers for the 5 μm wavelength range. While for the case where the AWG is used for QCL/ICL laser multiplexing only TM polarization operation needs to be considered, for the case of the midIR spectrometer both TE and TM polarization will be analyzed as a first step towards polarization insensitive operation.

Manuscript received June 14, 2013; revised July 16, 2013; accepted July 31, 2013. Date of publication August 2, 2013; date of current version August 21, 2013. This work was carried out in the framework of FP7-ERC project MIRACLE. The work of Y. Shimura was supported by the FWO under a Pegasus Marie Curie Fellowship.

A. Malik, M. Muneeb, S. Pathak, and G. Roelkens are with the Photonics Research Group, Ghent University, Ghent 9000, Belgium (e-mail: aditya.malik@intec.ugent.be; muhammad.muneeb@intec.ugent.be; shibnath.pathak@intec.ugent.be; gunther.roelkens@intec.ugent.be).

Y. Shimura, J. Van Campenhout, and R. Loo are with imec, Leuven 3001, Belgium (e-mail: shimura@imec.be; jvcampen@imec.be; loo@imec.be).

Color versions of one or more of the figures in this letter are available online at http://ieeexplore.ieee.org.

Digital Object Identifier 10.1109/LPT.2013.2276479

II. Germanium-on-Silicon Waveguide Platform

A 2 μm thick epitaxial layer of germanium is grown on an n-type Si(001) substrate at imec on 200 mm wafers by an atmospheric chemical vapor deposition system as described in [9]. Since there is a lattice mismatch of 4.2% between Si and Ge, the threading dislocation density (TDD) in the Ge

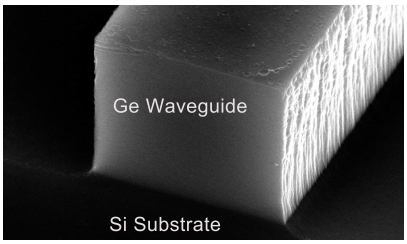

Fig. 1. Cleaved facet of a germanium-on-silicon waveguide.

layer is quite high. To reduce this TDD in the film, the grown germanium is annealed at 850 °C for 3 minutes which results in a TDD of $10^7 cm^{-2}$.

To define Ge-on-Si photonic integrated circuits, a Ti/Cr metal mask is defined by means of a lift-off approach using i-line contact lithography. The lift-off process introduces a roughness on the waveguide sidewalls, as can be seen in the scanning electron microscope image in Figure 1. This is however not detrimental for the operation of the devices as will be shown in this letter. Normally, a resist or a dielectric mask would be preferred to define patterns but since the etching chemistry used for germanium etches these masks at a faster rate, a metal mask is to be used. The dry etching of germanium is carried out in a CF_4/O_2 plasma, followed by an HF dip to remove the metal mask. The waveguides are etched completely through the 2 μm thick germanium device layer and are air clad. The waveguide structures were cleaved after thinning down the silicon substrate to 400 μm.

III. AWG Design

An AWG consists of two slab regions (known as free propagation regions (FPRs) or star couplers) and an array of waveguides with a constant length increment between them (known as delay lines). When light enters the input star coupler through a waveguide, it diverges and gets coupled in the array of waveguides. The length difference ΔL between two consecutive waveguides is such that the optical path length difference is equal to an integral multiple of the central wavelength (λ_c) of the (de)multiplexer ($\Delta L = m\lambda_c/n_{eff}$, where m is the diffraction order and n_{eff} is the effective index of the mode in the array waveguide). The free spectral range (FSR) of the (de)multiplexer is given by $\lambda^2/(n_g \Delta L)$, where n_g is the group index of the mode in the array waveguide. By placing the output waveguides at the output star coupler, spatial filtering of wavelengths can be achieved. More details about the basic theory of AWGs can be found in [10]. Details on the specific design strategy used in this work can be found in [11]. We designed an AWG with 200 GHz (18 nm) channel spacing with five channels (146 nm free spectral range). The waveguide aperture was 4 μm while the waveguide pitch was 5 μm (the 1 μm gap between waveguides is limited by the i-line lithography). The AWG contained 36 waveguides arms and the path length difference between the delay lines was 46 μm. For the waveguides used in the array, which were broadened to a width of 4 μm in order to minimize the phase noise which could arise from side wall roughness, the effective index was 3.52 for TE polarization and 3.49 for TM polarization while the group index was 4.12 and 4.15 respectively. Figure 2 (a) shows a microscopic image of the complete fabricated device while Figure 2 (b) shows a SEM image of the input star coupler of the fabricated AWG. The footprint of the complete device is 1 mm by 1 mm.

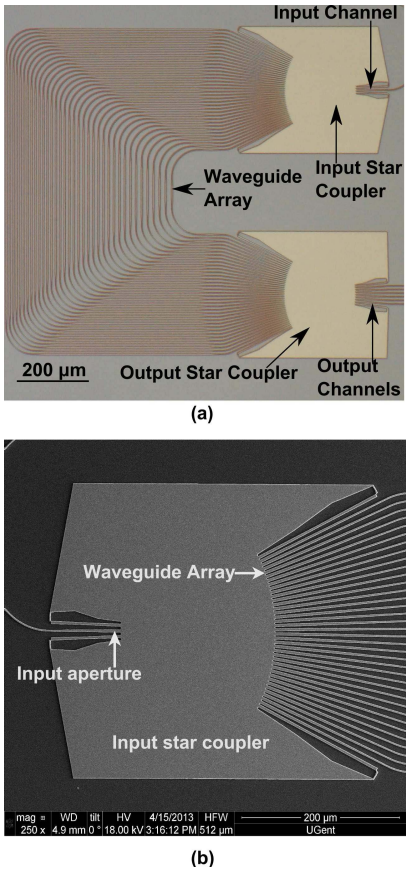

Fig. 2. (a) A microscope image of the fabricated AWG showing different sections and (b) a SEM picture of the input section specifying the input aperture, input star coupler and the array waveguides.

IV. Measurement Setup

A schematic diagram of the measurement setup is shown in Figure 3. Light was coupled from a widely tunable quantum cascade laser (Daylight Solutions) in a single mode Indium Fluoride fiber (IRPhotonics) using a chalcogenide aspheric lens (Thor Labs). A MgF_2 Babinet-Soleil polarization controller was used to choose the desired polarization in fiber. The output power of the laser is 60 mW of which 7.5 mW is coupled in the fiber at 5.3 μm. The cleaved end of the fiber was mounted on a piezo-driven xyz stage to align accurately with the input taper waveguide. The insertion loss from fiber to tapered waveguide, found by comparing the tip-to-tip transmission with transmission through a straight waveguide, was found to be approximately 7.5 dB for both polarizations. Light from the output taper was collected again using a cleaved fiber mounted on a piezo-driven xyz stage and then coupled to an InSb detector. To improve the signal to noise ratio, the output of the detector was coupled to a lock-in amplifier. For these measurements the laser was operated in pulsed mode at 100 kHz repetition frequency with a duty cycle

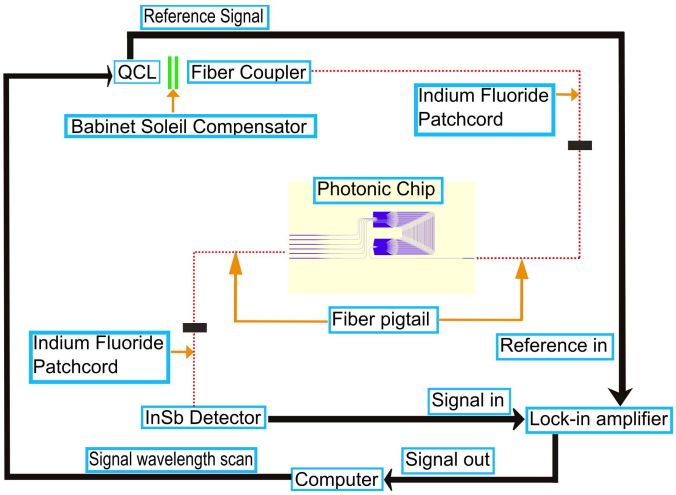

Fig. 3. Schematic diagram of the measurement setup.

of 5% and the trigger from the laser was used as reference for the lock-in amplifier. The laser and lock-in amplifier are addressed by software to scan the wavelength and record the corresponding output simultaneously.

V. Waveguide Losses

Waveguide spirals of different lengths (0.5 cm, 1 cm, 2 cm and 3 cm) were fabricated. The waveguides were 2.2 μm wide providing single mode operation in the 5−5.4 μm wavelength range for both polarizations. We simulated the bend losses using a full-vectorial eigenmode expansion tool FIMMWAVE in these Ge-on-Si waveguides and found that a radius of 100 μm is large enough to avoid any bend losses. The waveguide losses were measured using a cut-back method. Figure 4 shows the waveguide losses at a fixed wavelength of 5.4 μm for TE and TM polarization while Figure 5 shows waveguide losses in the range of 2.5–3.5 dB/cm for TE polarized light and 3–4 dB/cm for TM polarized light in the 5.15–5.45 μm wavelength range. These low losses are related to the thick germanium waveguiding layer which reduces the overlap of the optical mode with the defective Ge/Si interface.

VI. AWG Measurement Results

Figure 6 (a) and Figure 6 (b) show the normalized transmission spectrum of the 5 × 200 GHz channel spacing AWG for TE and TM polarized light respectively. The measured spectra are normalized with respect to a straight waveguide containing two tapers for in and out coupling and a single mode waveguide of length 0.5 cm present next to the device. This normalization is carried out in order to eliminate the coupling loss from fiber to waveguide and analyze the performance of device itself. For calibrating the polarization, we adjusted the Babinet-Soleil compensator for each measurement of a channel transmission such that the transmission peak due to the orthogonal polarization was minimized. The side lobe cross-talk is around 20 dB for TE polarization and is around 16 dB for TM polarization. The polarization dependent shift in peak wavelength of channels is found to be 51 nm.

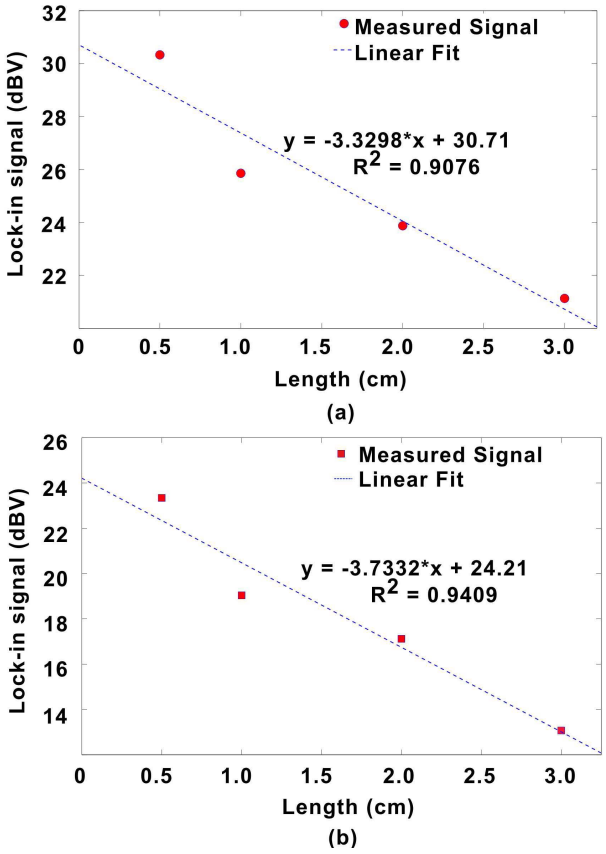

Fig. 4. Cut-back measurements at 5.4 μm wavelength for (a) TE polarization and (b) TM polarization (2.2 μm wide germanium-on-silicon waveguides).

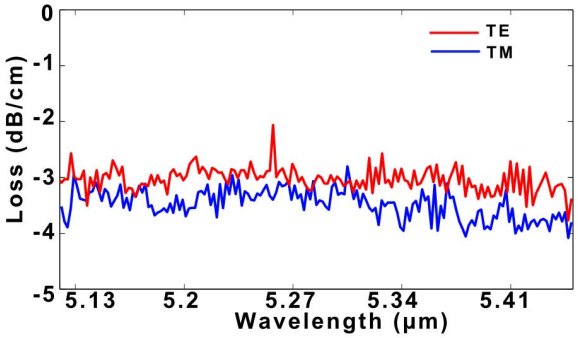

Fig. 5. Waveguide loss for TE and TM polarized light as a function of wavelength (2.2 μm wide germanium-on-silicon waveguides).

To calculate the insertion loss of the device, we did a fit of the central channel with a gaussian function as shown in Fig. 6. From this fit, an insertion loss of −2.5 dB is found for TE polarized light and −3.1 dB for TM polarized light. These values of cross talk and insertion loss are comparable to the silicon-on-insulator AWG operating at 3.8 μm reported in [5] despite of the fact that the AWG reported in this letter is fabricated using i-line contact lithography which restricts the minimum definable feature size to 1 μm. For the application as wavelength multiplexer for DFB laser arrays the most important metric is insertion loss. Insertion losses in the range of 2 to 3 dB outperform the theoretically achievable insertion loss of light combiners e.g. based on multimode interference

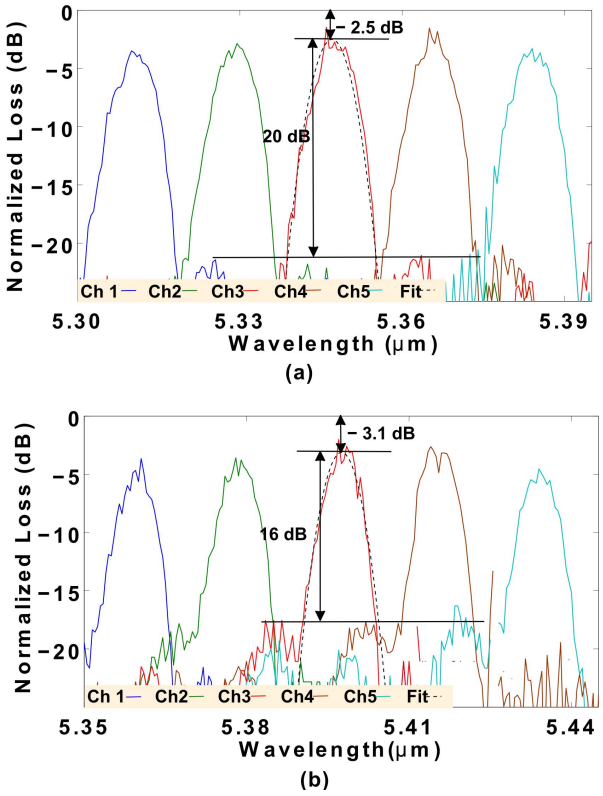

Fig. 6. Normalized transmission spectrum of the 5×200 GHz AWG for (a) TE polarized light and (b) TM polarized light.

couplers ($10\log_{10}5$ dB = 7 dB), showing the potential of these devices for the low loss multiplexing of large arrays of DFB lasers. The 16–20 dB crosstalk is also promising for the use of such devices as integrated spectrometers, although the polarization dependent wavelength shift still needs to be minimized for proper polarization insensitive operation. One way of solving this problem is to employ a rib type waveguide and apply the methods as described in [12]. For fully etched devices, a Si cladding could be grown on a square shaped waveguide such that the effective index of TE and TM modes becomes equal and there is no polarization dependent shift.

VII. Conclusion

We demonstrate the use of AWGs as wavelength multiplexers on the germanium-on-silicon platform in the mid-infrared for the first time. These devices can become enabling components for the realization of mid-infrared light engines and spectrometers that cover a wide wavelength range, are compact, rugged and cheap. This might pave the way to a whole new class of applications for spectroscopic sensing systems, which so far could not be addressed due to the lack of commodity versatile mid-infrared light engines and spectrometers.

References

[1] R. F. Curl, *et al.*, "Quantum cascade lasers in chemical physics," *Chem. Phys. Lett.*, vol. 487, nos. 1–3, pp. 1–18, 2010.

[2] B. G. Lee, *et al.*, "DFB quantum cascade laser arrays," *IEEE J. Quantum Electron.*, vol. 45, no. 5, pp. 554–565, May 2009.

[3] B. G. Lee, *et al.*, "Beam combining of quantum cascade laser arrays," *Opt. Express*, vol. 17, no. 18, pp. 16216–16224, 2009.

[4] R. Soref, "Mid-infrared photonics in silicon and germanium," *Nat. Photon.*, vol. 4, no. 8, pp. 495–497, 2010.

[5] M. Muneeb, *et al.*, "Demonstration of silicon on insulator mid-infrared spectrometers operating at 3.8 um," *Opt. Express*, vol. 21, no. 10, pp. 11659–11669, 2013.

[6] Y.-C. Chang, V. Paeder, L. Hvozdara, J.-M. Hartmann, and H. P. Herzig "Low-loss germanium strip waveguides on silicon for the mid-infrared," *Opt. Lett.*, vol. 37, no. 14, pp. 2883–2885, 2012.

[7] Y. Xia, C. Qiu, X. Zhang, W. Gao, J. Shu, and Q. Xu "Suspended Si ring resonator for mid-IR application," *Opt. Lett.*, vol. 38, no. 7, pp. 1122–1124, 2013.

[8] T. B. Jones, *et al.*, "Silicon-on-sapphire integrated waveguides for the mid-infrared," *Opt. Express*, vol. 18, no. 12, pp. 12127–12135, 2010.

[9] R. Loo, *et al.*, "High quality Ge virtual substrates on Si wafers with standard STI patterning," *J. Electr. Soc.*, vol. 157, no. 1, pp. H13–H21, 2010.

[10] M. Smit and C. Van Dam, "PHASAR-based WDM-devices: Principles, design and applications," *IEEE J. Sel. Topics Quantum Electron.*, vol. 2, no. 2, pp. 236–250, Jan. 1996.

[11] S. Pathak, M. Vanslembrouck, P. Dumon, D. Van Thourhout, and W. Bogaerts, "Optimized silicon AWG with flattened spectral response using an MMI aperture," *J. Lightw. Technol.*, vol. 31, no. 1, pp. 87–93, Jan. 1, 2013.

[12] L. Vivien, S. Laval, B. Dumont, S. Lardenois, A. Koster, and E. Cassan "Polarization-independent single-mode rib waveguides on silicon-on-insulator for telecommunication wavelengths," *Opt. Commun.*, vol. 210, nos. 1–2, pp. 43–49, 2002.